

Synthesis and evaluation of two fluorine-18 labelled phenylbenzothiazoles as potential *in vivo* tracers for amyloid plaque imaging

K. Serdons,^{a*} D. Vanderghinste,^b M. Van Eeckhoudt,^a P. Borghgraef,^c H. Kung,^d F. Van Leuven,^c T. de Groot,^b G. Bormans,^a and A. Verbruggen^a

Uncharged derivatives of thioflavin-T have known *in vitro* and *in vivo* affinity for amyloid β . We synthesized and evaluated two derivatives with a fluorine-18 labelled fluoropropoxy substituent either at the 6-position or at the 2'-position of the 2-(4'-aminophenyl)-1,3-benzothiazole core with the aim to get suitable radiotracers to perform amyloid plaque imaging. The fluorine-18 labelled compounds were obtained by nucleophilic substitution of the corresponding tosyl precursors with [¹⁸F]fluoride with a radiochemical yield of 50%, yielding 6-(3'-[¹⁸F]fluoropropoxy)-2-(4'-aminophenyl)-1,3-benzothiazole ([¹⁸F]2) and 2-[2'-(3'-[¹⁸F]fluoropropoxy)-4'-aminophenyl]-1,3-benzothiazole ([¹⁸F]3) with a specific activity between 33 and 51 GBq/ μ mol. The identity of the radiolabelled compounds was confirmed using radio-LC-MS and by comparing retention times on RP-HPLC. Biodistribution studies in healthy mice showed for both compounds a relatively high initial brain uptake, which was significantly higher for [¹⁸F]2 than for [¹⁸F]3 (4.5% ID/g versus 3.0% ID/g, $p < 0.05$). Wash-out from control brain was faster for [¹⁸F]3. *In vitro* binding affinity tests using human AD brain homogenates revealed that only compound 2 has affinity for fibrillar amyloid β ($K_i = 14.5$ nM). This was confirmed by the incubation of transgenic APP mouse brain sections with the cold compounds, where 3 did not stain any structure whereas 2 stained amyloid plaques present in APP mouse brain. These data suggest that [¹⁸F]2 may be a useful tracer for *in vivo* visualization of fibrillar amyloid β .

Keywords: amyloid; diagnosis; PET; fluorine-18; phenylbenzothiazole

Introduction

Fibrillar amyloid β (A β) is an aggregated protein found in brain of patients suffering from Alzheimer's disease (AD). Therefore, *in vivo* visualization of the presence of this protein in the brain using single photon emission computed tomography (SPECT) or positron emission tomography (PET) with an appropriate radiopharmaceutical would allow early diagnosis of this disorder and evaluation of therapies aiming to reduce the amyloid β burden.

Several radiolabelled imaging agents binding specifically to A β have already been reported (Figure 1).¹ The first synthesized compounds were derived from Congo red or chrysamine G, dyes useful for staining fibrillar amyloid *in vitro*,^{2–5} and derivatives of styrylbenzene such as X-34,³ BSB,^{4–9} ISB and IMSB.⁷ These agents have a rather high molecular mass and are ionized at physiological pH, impairing their ability to cross the blood–brain barrier (BBB) by passive diffusion. Smaller derivatives consisting of about half the structure of X-34 and lacking the ionizable groups have been developed. These are labelled with either carbon-11 (N-[¹¹C]methylamino-4'-hydroxystilbene, SB-13) or iodine-125 (N,N-dimethylamino-3'-[¹²⁵I]iodostilbene).^{8,9} Contrary to the chrysamine G and X-34 derivatives, these stilbenes show a high initial brain uptake in healthy mice and a nanomolar affinity for fibrillar amyloid β *in vitro*. Barrio *et al.* investigated fluorine-18 labelled derivatives of FDDNP as potential tracers for *in vivo* visualization of fibrillar amyloid β .¹⁰ They found that these

compounds bind not only to senile plaques but also to neurofibrillary tangles, another hallmark of AD. Patient studies have shown the ability of these compounds to detect pathological deposits in the brain of AD patients.¹¹ Other promising tracer agents for *in vivo* imaging of amyloid pathology are an iodine-125 labelled N,N-dimethylamino-fluorene,¹² the carbon-11 labelled PIB (see *infra*) and the fluorine-18 labelled styrylbenzoxazole BF-168,¹³ acridine orange analog BF-108¹⁴ and stilbene ¹⁸F-BAY94-9172.¹⁵

Over the last years, uncharged derivatives of thioflavin-T (ThT) have been synthesized and labelled with a variety of radioisotopes in the search for a radiolabelled probe for diagnosis of AD. ThT itself is positively charged due to the presence of a quaternary nitrogen atom and is not able to cross the BBB by

^aLaboratory for Radiopharmacy, K. U. Leuven, O&N2, Herestraat 49 - bus 821, 3000 Leuven, Belgium

^bRadiopharmacy, U. Z. Gasthuisberg, Herestraat 49, 3000 Leuven, Belgium

^cLaboratory of Experimental Genetics and Transgenesis, K. U. Leuven, O&N1, Herestraat 49 - bus 602, 3000 Leuven, Belgium

^dDepartment of Radiology, University of Pennsylvania, Market Street 3700 - room 305, Philadelphia, United States

*Correspondence to: K. Serdons, Laboratory for Radiopharmacy, Faculty of Pharmaceutical Sciences, K. U. Leuven, O&N2, Herestraat 49 - bus 821, 3000 Leuven, Belgium.

E-mail: Kim.serdons@pharm.kuleuven.be

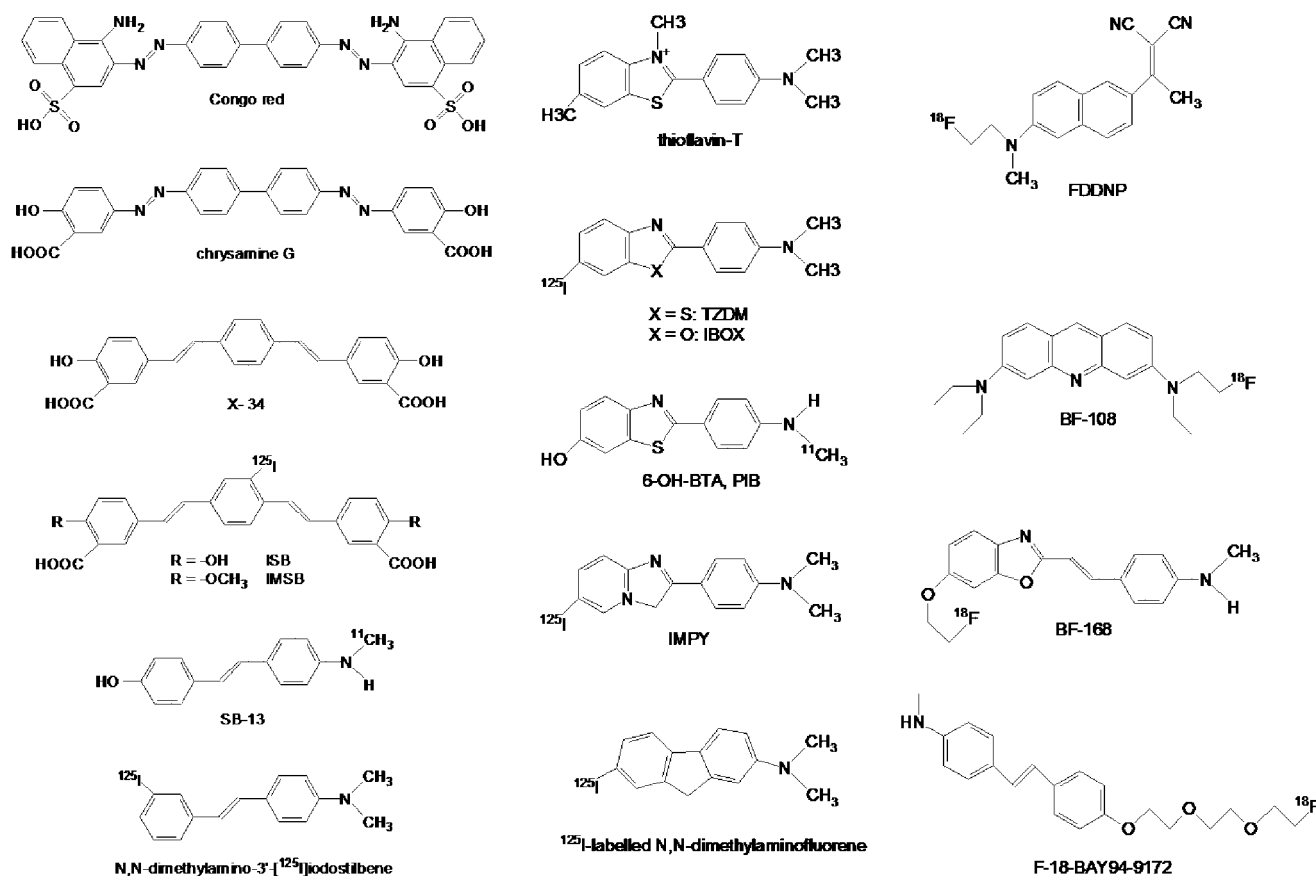


Figure 1. Structures of reported potential tracer agents for imaging of amyloid β .

passive diffusion. Klunk *et al.* reported that uncharged thioflavin-T derivatives bind with high affinity to fibrillar amyloid.¹⁶ Derivatives labelled with iodine-125 (^{125}I -TZDM¹⁰ and 2-(3'-[^{125}I]iodo-4'-aminophenyl)-6-hydroxybenzothiazole¹⁷) show high binding affinity for fibrillar amyloid β and are useful for *in vitro* experiments. Other compounds labelled with carbon-11 have also been developed, such as [^{11}C]6-Me-BTA-1, [^{11}C]6-Me-BTA-2 and [^{11}C]6-OH-BTA-1 with the latter, also known as Pittsburgh Compound-B or PIB, being the most promising tracer agent.^{18,19} The benzothiazole moiety is apparently not strictly necessary for binding affinity, as similar structures have been reported in which the benzothiazole core has been replaced, including a benzoxazole (IBOX),²⁰ a benzofuran²¹ and an imidazo[1,2-a]pyridine (IMPY)^{22,23} that bind with high affinity to fibrillar amyloid β . Mathis *et al.* recently reported an ^{18}F -labelled ThT derivative and are evaluating this compound as potential amyloid imaging agent.²⁴ We already reported several ^{18}F -labelled phenylbenzothiazoles with the ^{18}F -atom directly attached to the 2-phenyl ring.^{25,26} In the present study, we report the synthesis, labelling and (biological) evaluation of two phenylbenzothiazoles with a fluorine-18 labelled fluoropropoxy substituent as potential PET-tracers for fibrillar amyloid β .

Results and discussion

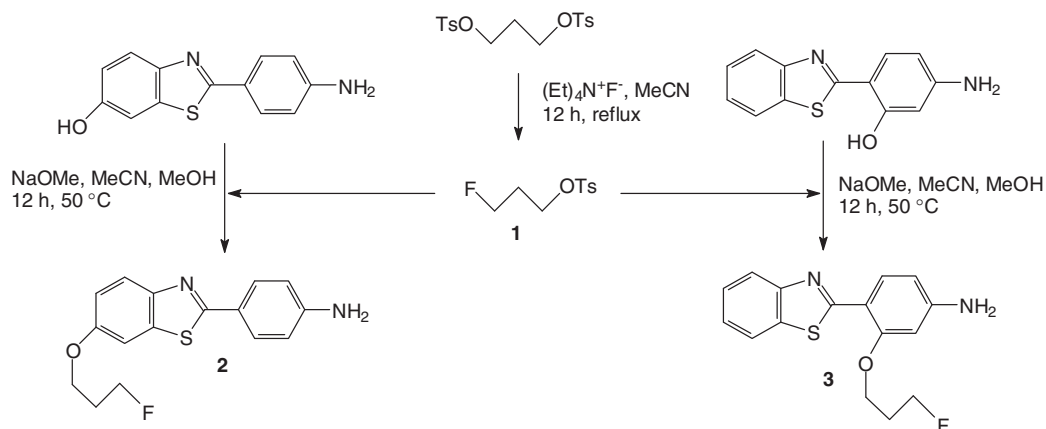
Chemistry

6-Hydroxy-2-(4'-aminophenyl)-1,3-benzothiazole and 2-(2'-hydroxy-4'-aminophenyl)-1,3-benzothiazole were synthesized

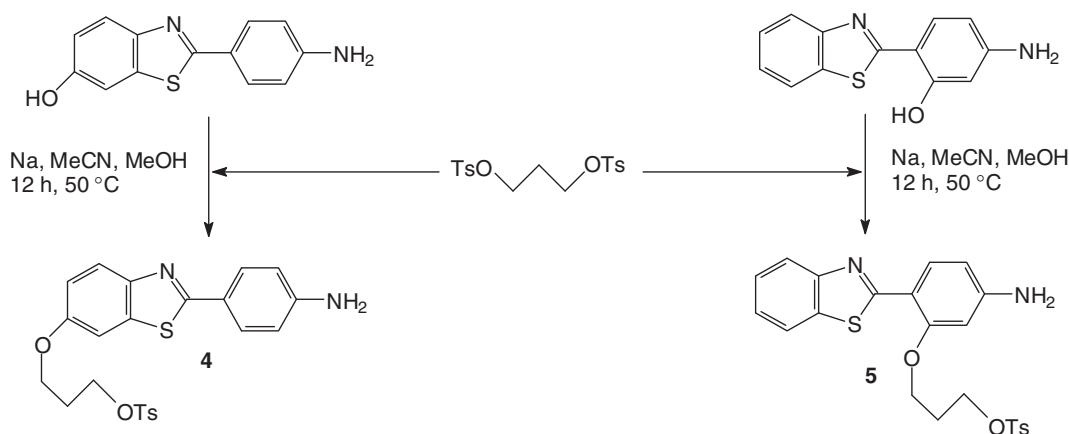
using a modification of a method described by Shi and co-workers.²⁷

For the synthesis of the non-radioactive 3-fluoropropoxy derivatives 6-(3''-fluoropropoxy)-2-(4'-aminophenyl)-1,3-benzothiazole (**2**) and 2-[2'-(3''-fluoropropoxy)-4'-aminophenyl]-1,3-benzothiazole (**3**), 1,3-propanediol di-*p*-tosylate was mono-fluorinated via a nucleophilic substitution to get 3-fluoropropyltosylate (**1**), followed by reaction of this intermediate with the appropriate hydroxy substituted 2-(4'-aminophenyl)-1,3-benzothiazole (Scheme 1). For the synthesis of 3-fluoropropyltosylate **1**, tetraethylammonium fluoride was reacted with 1,3-propanediol di-*p*-tosylate in acetonitrile at reflux.²⁸ **1** was then used for reaction with the 6- or 2'-hydroxy-substituted precursors to yield **2** or **3**. The compounds were purified using silica gel column chromatography, followed by reversed phase medium pressure liquid chromatography (RP-MPLC), resulting in a chemical purity of more than 99%.

The synthesis of the precursors for fluorine-18 labelling, i.e. 2-[2'-(3''-*p*-tosyloxypropoxy)-4'-aminophenyl]-1,3-benzothiazole (**4**) and 6-(3''-*p*-tosyloxypropoxy)-2-(4'-aminophenyl)-1,3-benzothiazole (**5**) is depicted in Scheme 2. 1,3-Propanediol di-*p*-tosylate was reacted with 6-hydroxy-2-(4'-aminophenyl)-1,3-benzothiazole or 2-(2'-hydroxy-4'-aminophenyl)-1,3-benzothiazole in the presence of sodium methanolate. A two-fold excess of 1,3-propanediol di-*p*-tosylate was used to avoid reaction at both tosyl groups and this was further inhibited by adding 6-hydroxy-2-(4'-aminophenyl)-1,3-benzothiazole or 2-(2'-hydroxy-4'-aminophenyl)-1,3-benzothiazole slowly to the solution of 1,3-propanediol di-*p*-tosylate.



Scheme 1. Synthesis of 6-(3''-fluoropropoxy)-2-(4'-aminophenyl)-1,3-benzothiazole (**2**) and 2-[2'-(3''-fluoropropoxy)-4'-aminophenyl]-1,3-benzothiazole (**3**).



Scheme 2. Synthesis of 6-(3''-*p*-tosyloxypropoxy)-2-(4'-aminophenyl)-1,3-benzothiazole (**4**) and 2-[2'-(3''-*p*-tosyloxypropoxy)-4'-aminophenyl]-1,3-benzothiazole (**5**).

Radiolabelling

Labelling of the tosylated precursors **4** and **5** was done using the mixture $^{18}\text{F}/\text{K}_2\text{CO}_3/\text{kryptofix}^{\text{®}}$ 222 in anhydrous acetonitrile. The decay corrected radiochemical yield was about 50% for both compounds and the specific activity after purification using high performance liquid chromatography (HPLC) varied typically between 33 and 51 GBq/ μmol at the end of synthesis (EOS) in both cases.

Strong evidence of the identity of the radiolabelled compounds was obtained by comparing their retention times on HPLC with the retention times of the cold reference compounds and by using radio-LC-MS. Because of the low amounts of fluorine-18 labelled compound in the labelling reaction mixture, it was not possible to directly detect the radiolabelled compound. Instead, we detected the fluorine-19 labelled analogue, which is present in 1200 – 2000-fold excess in the labelling mixture. Nevertheless, this indirect method provided us confirmation of the identity of the radiolabelled compound, as the molecular mass of the fluorinated compound was not found in the mixture before, but only after labelling. A radio-LC-MS chromatogram of the labelling reaction mixture of $[^{18}\text{F}]\mathbf{2}$ after purification over two Seppak[®] Plus silica cartridges is shown in Figure 2. The accurate mass spectrum corresponding to the main peak in the radiometric signal (retention time 12.64 min, Figure 2b) shows a molecular ion mass of

303.0981 Da, corresponding to the theoretical molecular ion mass (303.0962 Da) of **2** (Figure 3). The single ion mass chromatogram of mass range 303.533 – 303.573 Da (Figure 2a) shows that the retention time of these ions is identical to that of the main peak in the radiometric signal, also indicating that the peak in the radiometric signal corresponds to $[^{18}\text{F}]\mathbf{2}$. The small peak at 7.35 min in the single ion mass chromatogram corresponds to the hydrolysed precursor. The tosylated precursor **4** elutes at 15.37 min. Similar results were obtained for the identity confirmation of $[^{18}\text{F}]\mathbf{3}$ using radio-LC-MS (data not shown). Identity confirmation was also done by comparison of the retention times of the authentic analogues **2** and **3** and ^{18}F -labelled $[^{18}\text{F}]\mathbf{2}$ and $[^{18}\text{F}]\mathbf{3}$, respectively, on HPLC.

Partition coefficient

The logP value, which was determined using a modification of the method described by Yamauchi and co-workers,²⁹ was 2.07 ± 0.06 for $[^{18}\text{F}]\mathbf{2}$ and 2.96 ± 0.05 for $[^{18}\text{F}]\mathbf{3}$, which is within the optimal range for free diffusion over the BBB.³⁰

Biodistribution in control mice

Table 1 shows the results of the biodistribution study of $[^{18}\text{F}]\mathbf{2}$ and $[^{18}\text{F}]\mathbf{3}$ in control mice. Both compounds show a

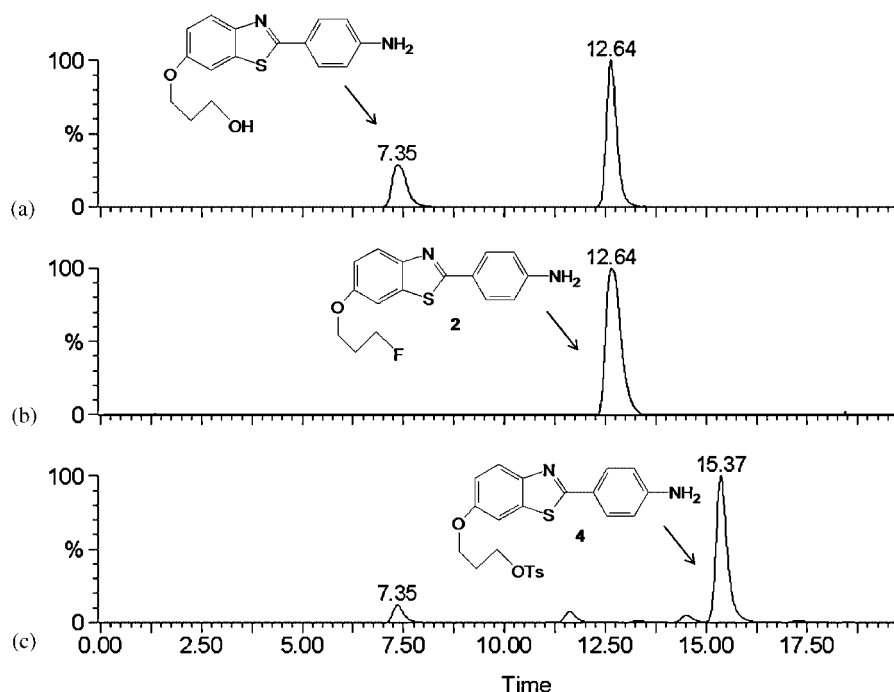


Figure 2. Radio-LC-MS analysis of the labeling reaction mixture of 6-(3'-[¹⁸F]fluoropropoxy)-2-(4'-aminophenyl)-1,3-benzothiazole ([¹⁸F]**2**) after elution over two Seppak[®] Plus silica cartridges. (a) Ion mass chromatogram of the ions in the mass range between 303.533 – 303.573 Da; (b) radiometric signal; and (c) UV signal at 365 nm.

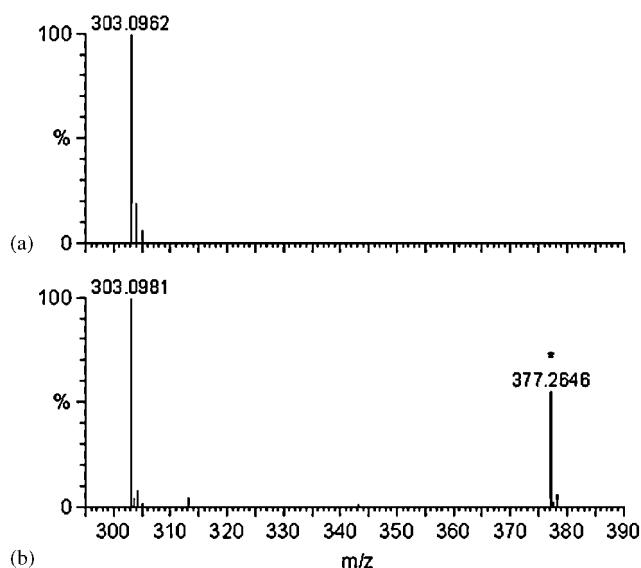


Figure 3. Accurate mass spectrum of [¹⁸F]**2** with kryptofix[®] 222 ($M_r = 377.2646$ Da) as lock mass. (a) Theoretical mass spectrum and (b) experimental mass spectrum with at 377.2646 the peak originating from kryptofix[®] 222.

significant initial brain uptake, which is the highest for [¹⁸F]**2** (2 min p.i.: [¹⁸F]**2**: 4.5% ID/g and [¹⁸F]**3**: 3.0% ID/g). Wash-out from brain is faster for [¹⁸F]**3** than for [¹⁸F]**2** and the ratio of the brain activity at 2 min p.i. versus 60 min p.i. is 4.5 for [¹⁸F]**3** and 3.8 for [¹⁸F]**2**, but the difference is not significant ($p > 0.05$). The rate of excretion through the renal pathway is for both tracer agents about the same, but the excretion through the hepatobiliary pathway is 3 times higher for [¹⁸F]**3** compared with [¹⁸F]**2** (60 min p.i.: [¹⁸F]**2**: 15.5% ID and [¹⁸F]**3**: 46.9% ID).

In vitro affinity for human fibrillar amyloid β

In order to obtain information on the *in vitro* affinity of these tracer agents for amyloid β fibrils, determination of their binding to homogenates of *post mortem* human AD brain is a useful test. The K_i value obtained for the non-radioactive compound **2** was 14.5 ± 4 nM, which is in the range ($K_i \leq 20$ nM) for good binding affinity for A β plaques. Surprisingly, position isomer **3** did not show any affinity for fibrillar A β in the tested concentration range. The obtained K_i value was more than 4000 nM for **3**. This lack of binding potential of **3** may be due to the fact that a derivatization at the 2'-position causes a torsion of the bond between carbon-2 and carbon-1', leading to a conformation of the phenylbenzothiazole that is not able to bind to amyloid. To our knowledge, all uncharged derivatives of thioflavin T with affinity for fibrillar amyloid β reported up to now are derivatized either at the 3'-position or at the benzothiazole moiety itself and not at the 2'-position.

In vitro affinity for amyloid present in mouse brain sections

We evaluated the binding potential of the two non-radioactive fluorinated compounds (**2** and **3**) for fibrillar amyloid β on *post mortem* brain sections of transgenic AD mice. The results of the incubation of 6 μ m microtome sections of transgenic APP mouse brain with either **2** or **3** in a 1 μ M concentration together with the immunohistochemical staining of neighbouring sections is shown in Figure 4. The region of the mouse brain shown is the subiculum, a structure located in the hippocampic region and rich in plaques in AD mice.

From Figure 4 it can be seen that **2** (top left) stains a few plaques in this region of the brain while **3** (top right) does not. This is consistent with the findings of the *in vitro* binding affinity test on homogenates of human AD brain. Comparison of the

images from the immunohistochemical staining (bottom) with the fluorescence staining shows that **2** stains less fibrillar A β than the pan A β does, probably because of the higher affinity of the antibodies for fibrillar A β . Owing to the few potential

plaques that were stained with **2** at this concentration, no colocalization was possible.

Experimental section

Instruments and general conditions

All reagents and solvents used in synthesis were purchased from Acros Organics (Geel, Belgium), Fluka (Bornem, Belgium) or Aldrich (Sigma-Aldrich, Bornem, Belgium) and were used without further purification. MgSO₄ was used as drying agent. Column purification of reaction mixtures was done using silica gel with a particle size between 0.04 and 0.063 mm (230 – 400 mesh) (MN Kieselgel 60 M, Macherey Nagel, Düren, Germany) or by medium pressure liquid chromatography (MPLC). Thin layer chromatography (TLC) was carried out using precoated silica TLC plates (DC-Alufohlen-Kieselgel, Fluka, Buchs, Switzerland). The structure of the synthesized products was confirmed with ¹H-nuclear magnetic resonance (NMR) spectroscopy on a Gemini 200 MHz spectrometer (Varian, Palo Alto, CA, USA). Chemical shifts are reported as δ -values (parts per million) relative to tetramethylsilane ($\delta=0$). Coupling constants are reported in hertz. Splitting patterns are defined by s (singlet), d (doublet), dd (double doublet), t (triplet), q (quartet) and m (multiplet). For melting point determination, an Electrothermal IA9000 digital melting point apparatus was used (Electrothermal, Southend-on-Sea, England).

Batches of [¹⁸F]fluoride were prepared by an ¹⁸O(p,n)¹⁸F reaction by irradiation of 500 μ l of 97% ¹⁸O-enriched water (Rotem HYOX¹⁸, Rotem Industries, Beer Sheva, Israel) in a titanium target with 10 MeV protons using an IBA Cyclone 10/5

	% ID \pm σ		% ID/g \pm σ	
	2 min p.i.	60 min p.i.	2 min p.i.	60 min p.i.
[¹⁸F]2				
Urine	0.1 \pm 0.1	7.2 \pm 0.5	—	—
Kidneys	5.0 \pm 0.8	1.3 \pm 0.4	8.3 \pm 0.6	2.2 \pm 0.4
Liver	20.6 \pm 1.5	4.1 \pm 0.8	10.7 \pm 1.5	1.9 \pm 0.4
Intestines	10.3 \pm 0.7	11.4 \pm 1.7	—	—
Stomach	1.6 \pm 0.8	0.7 \pm 0.5	—	—
Cerebrum	1.5 \pm 0.4	0.4 \pm 0.0	4.5 \pm 0.8	1.2 \pm 0.0
Cerebellum	0.5 \pm 0.1	0.2 \pm 0.0	4.6 \pm 0.8	1.4 \pm 0.2
Blood	6.9 \pm 0.8	3.1 \pm 0.6	2.7 \pm 0.3	1.1 \pm 0.2
[¹⁸F]3				
Urine	0.3 \pm 0.2	5.5 \pm 3.4	—	—
Kidneys	5.8 \pm 2.5	1.8 \pm 1.0	9.0 \pm 3.3	3.5 \pm 1.9
Liver	17.2 \pm 1.6	7.5 \pm 1.0	7.6 \pm 1.2	4.5 \pm 0.6
Intestines	8.6 \pm 0.7	39.4 \pm 10.6	—	—
Stomach	1.6 \pm 0.3	2.4 \pm 2.5	—	—
Cerebrum	0.9 \pm 0.1	0.2 \pm 0.1	3.0 \pm 0.3	0.6 \pm 0.3
Cerebellum	0.3 \pm 0.1	0.1 \pm 0.1	3.2 \pm 0.2	0.7 \pm 0.3
Blood	9.4 \pm 2.5	1.1 \pm 0.6	3.4 \pm 0.9	0.5 \pm 0.3

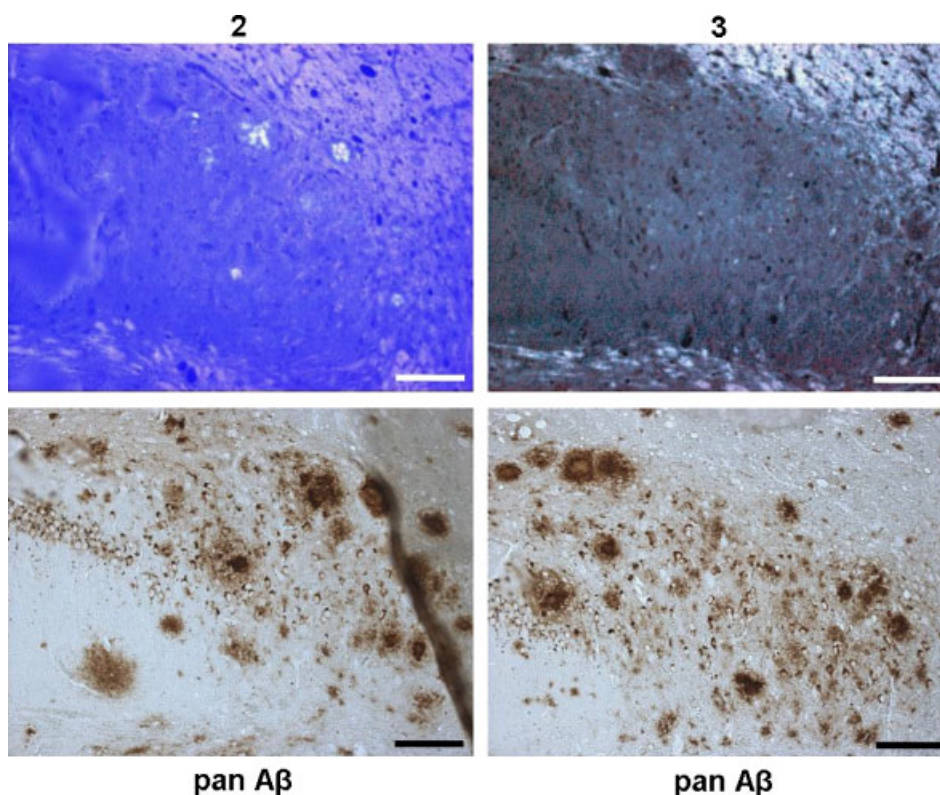


Figure 4. Fluorescence microscopic images after incubation of transgenic AD mouse brain microtome sections with **2** (top left) and **3** (top right). Neighbouring sections were immunohistochemically stained with pan A β (bottom images). Bar = 100 μ m.

cyclotron (IBA, Louvain-la-Neuve, Belgium). Quantitative determination of radioactivity in samples was done using an automatic gamma counter coupled to a multi-channel analyzer (Wallac 1480 Wizard[®] 3'', Wallac, Turku, Finland). The data were corrected for physical decay and background radiation.

Combined liquid chromatography and mass spectrometry (LC-MS) was performed on a system consisting of a Waters Alliance 2690 separation module (Waters, Milford, MA, USA) coupled to an XTerra[®] MS C18 3.5 μ m 2.1 mm \times 50 mm reverse phase high performance liquid chromatography (RP-HPLC) column (Waters). The mobile phase consisted of a mixture of acetonitrile (MeCN, A) and 0.1% ammonium acetate (B) with a linear gradient of 30 A:70 B v/v to 80 A:20 B v/v in 20 min at a flow rate of 300 μ l/min. The eluate was first led through a UV-spectrometer (Waters 2487 Dual λ absorbance detector) and subsequently over a 3-inch NaI(Tl)-crystal coupled to a single channel analyzer (The Nucleus, Oak Ridge, TN, USA) for radiometric detection before it was injected in a time-of-flight mass spectrometer (LCT, Micromass, Manchester, England) equipped with a standard electrospray ionization (ESI) probe. Accurate mass determination was done by co-injection of a kryptofix[®] 222-solution by means of a Harvard 22 syringe pump (Harvard Instruments, Holliston, USA). Acquisition and processing of data was done with Masslynx software (Version 3.5).

RP-HPLC was done with a system consisting of a Merck-Hitachi ternary pump connected with a Waters 2487 dual wavelength absorbance detector and a 3-inch NaI(Tl) crystal connected with an EG&G Ortec ACEMate[™] model 925-scint single channel analyzer (EG&G Ortec, Oak Ridge, TN, USA).

Gas chromatography was performed with a DI 200 gas chromatograph (Delsi Instruments, Suresnes, France) with a Porapak[®] QS 80/100 column (Alltech, Deerfield, IL, USA) of 180 cm \times 0.25 inch.

Animal experiments were performed according to the Belgian code of practice for the care and use of animals, after approval from the university ethics committee for animals.

Syntheses

3-Fluoropropyltosylate (1)

A solution of dry tetraethylammonium fluoride (745 mg, 5 mmol) (dried via repeated azeotropic evaporation of a solution in acetonitrile) in 20 ml anhydrous acetonitrile was added to a refluxing solution of 1,3-propanediol di-*p*-tosylate (1.92 g, 5 mmol) in 20 ml acetonitrile. Refluxing was continued for 12 h. The obtained suspension was filtered and the filtrate was evaporated under reduced pressure. The residue was purified using silica gel column chromatography with a mixture of CH₂Cl₂/hexane (50:50 v/v) as the eluent to yield 315 mg (1.36 mmol, 26.7%) of pure compound **1** in the form of an oil. ¹H-NMR (CDCl₃, 200 MHz): δ 2.04 (2H, dq, ⁴J_(H,F) = 25.8 Hz, CH₂-CH₂-CH₂); δ 2.46 (3H, s, CH₃); δ 4.16 (2H, t, FCH₂-CH₂-CH₂O); δ 4.49 (2H, dt, ³J_(H,F) = 46.8 Hz, FCH₂-CH₂-CH₂O); δ 7.36 (2H, d, ³J = 8.6 Hz, 3-H 5-H); δ 7.80 (2H, d, ³J = 8.0 Hz, 2-H 6-H).

6-(3''-Fluoropropoxy)-2-(4'-aminophenyl)-1,3-benzothiazole (2)

To a dispersion of 6-hydroxy-2-(4'-aminophenyl)-1,3-benzothiazole (242 mg, 1 mmol) in 2 ml of a mixture of acetonitrile and methanol (MeOH) (9:1 v/v) was added NaOMe (1.1 mmol) in 2 ml of a mixture of acetonitrile and methanol (8:2 v/v). The mixture

was slowly added to a vial containing **1** (232 mg, 1 mmol) in 2 ml acetonitrile/methanol (9:1 v/v) at 50°C. After 12 h the solvent was evaporated under reduced pressure. The residue was purified using silica gel column chromatography with CH₂Cl₂ as eluent, followed by RP-MPLC purification using LiChroprep RP 18 (Merck) as stationary phase and acetonitrile/0.1 % ammonium acetate (50:50 v/v) as mobile phase at a flow rate of 17 ml/min. UV absorption was monitored at 254 nm. Acetonitrile was evaporated under reduced pressure. The white precipitate formed was filtered off and dried in a vacuum oven. 94 mg (0.31 mmol, 31.1%) of the desired compound **2** was directly obtained as a white powder. ¹H-NMR (CDCl₃, 200 MHz): δ 2.21 (2H, dq, ⁴J_(H,F) = 26 Hz, CH₂-CH₂-CH₂); δ 4.16 (2H, t, FCH₂-CH₂-CH₂O); δ 4.68 (2H, dt, ³J_(H,F) = 47.4 Hz, FCH₂-CH₂-CH₂O); δ 6.73 (2H, d, ³J = 8.4 Hz, 3'-H 5'-H); δ 7.04 (1H, d, ³J = 8.8 Hz, 5-H); δ 7.33 (1H, s, 7-H); δ 7.84 (2H, d, ³J = 8.4 Hz, 2'-H 6'-H); δ 7.87 (1H, d, ³J = 9.2 Hz, 4-H). Accurate MS ES⁺ *m/z* [M+H]⁺ 303.0943 (calculated for C₁₆H₁₆FN₂OS 303.0962). Mp: 149.5–150.5°C.

2-[2'-(3''-Fluoropropoxy)-4'-aminophenyl]-1,3-benzothiazole (3)

A similar procedure as for the synthesis of **2** was used, starting from 2-(2'-hydroxy-4'-aminophenyl)-1,3-benzothiazole (242 mg, 1 mmol) and yielding 59.6% of **3**. ¹H-NMR (CDCl₃, 200 MHz): δ 2.39 (2H, dq, ⁴J_(H,F) = 26 Hz, CH₂-CH₂-CH₂); δ 4.27 (2H, t, FCH₂-CH₂-CH₂O); δ 4.81 (2H, dt, ³J_(H,F) = 47 Hz, FCH₂-CH₂-CH₂O); δ 6.29 (1H, s, 3'-H); δ 6.42 (1H, d, ³J = 8.8 Hz, 5'-H); δ 7.31 (1H, dd, ³J = 7.5 Hz, 6-H); δ 7.45 (1H, dd, ³J = 7.7 Hz, 5-H); δ 7.87 (1H, d, ³J = 7.8 Hz, 6'-H); δ 8.01 (1H, d, ³J = 8.0 Hz, 7-H); δ 8.39 (1H, d, ³J = 8.4 Hz, 4-H). Accurate MS ES⁺ *m/z* [M+H]⁺ 303.0943 (calculated for C₁₆H₁₆FN₂OS 303.0962). Mp: 140.5–141°C.

6-(3''-p-Tosyloxypropoxy)-2-(4'-aminophenyl)-1,3-benzothiazole (4)

To a dispersion of 6-hydroxy-2-(4'-aminophenyl)-1,3-benzothiazole (1.817 g, 7.5 mmol) in 15 ml of a mixture of acetonitrile and methanol (9:1 v/v) was added Na (190 mg, 8.25 mmol) dissolved in a mixture of 3 ml methanol and 12 ml acetonitrile. The resulting mixture was added to a dispersion of 1,3-propanediol di-*p*-tosylate (768 mg, 15 mmol) in 75 ml of a mixture of acetonitrile and methanol (9:1 v/v) and the reaction mixture was heated to 50°C for 12 h. The formed suspension was filtered off and the solvent removed from the filtrate by vacuum evaporation. The residue was purified using silica gel column chromatography with a mixture of CH₂Cl₂ and methanol (99:1 v/v) as eluent to obtain **4** (896 mg, 1.97 mmol, 26.3%) as a yellow-brown powder. ¹H-NMR (CDCl₃, 200 MHz): δ 2.14 (2H, m, CH₂-CH₂-CH₂); δ 2.30 (3H, s, CH₃); δ 3.98 (2H, t, OCH₂-CH₂-CH₂); δ 4.27 (2H, t, CH₂-CH₂OTs); δ 6.73 (2H, d, ³J = 8.8 Hz, 3'-H 5'-H); δ 6.87 (1H, d, ³J = 8.8 Hz, 5-H); δ 7.16 (1H, s, 7-H); δ 7.20 (2H, d, ³J = 8.0 Hz, 2''-H 6''-H); δ 7.75 (2H, d, ³J = 7.6 Hz, 3''-H 5''-H); δ 7.83 (1H, d, ³J = 9.0 Hz, 4-H); δ 7.84 (2H, d, ³J = 8.8 Hz, 2'-H 6'-H). Accurate MS ES⁺ *m/z* [M+H]⁺ 455.1067 (calculated for C₂₃H₂₃N₂O₄S₂ 455.1094). Mp: 129.5–130.5°C.

2-[2'-(3''-p-Tosyloxypropoxy)-4'-aminophenyl]-1,3-benzothiazole (5)

The same procedure as for the synthesis of **4** was used starting from 2-(2'-hydroxy-4'-aminophenyl)-1,3-benzothiazole (1.21 g, 5 mmol) and yielding 64.4% of **5**. ¹H-NMR (CDCl₃, 200 MHz): δ

2.17 (3H, s, CH₃); δ 2.31 (2H, m, CH₂CH₂CH₂); δ 4.01 (2H, t, OCH₂CH₂CH₂); δ 4.43 (2H, t, CH₂CH₂OTs); δ 6.16 (1H, s, 3'-H); δ 6.40 (1H, d, ³J=8.0 Hz, 5'-H); δ 6.98 (2H, d, ³J=8.2 Hz, 3''-H 5''-H); δ 7.31 (1H, dd, ³J=7.6 Hz, 6-H); δ 7.45 (1H, dd, ³J=6.9 Hz, 5-H); δ 7.64 (2H, d, ³J=8.4 Hz, 2''-H 6''-H); δ 7.81 (1H, d, ³J=7.8 Hz, 6'-H); δ 7.99 (1H, d, ³J=7.6 Hz, 7-H); δ 8.30 (1H, d, ³J=8.4 Hz, 4-H). Accurate MS ES⁺ *m/z* [M+H]⁺ 455.1064 (calculated for C₂₃H₂₃N₂O₄S₂ 455.1094). Mp: 130.5–132°C.

Radiolabelling

A Seppak[®] Light Accell[™] plus QMA anion exchange column (Waters) was rinsed with 10 ml of a 0.5 M K₂CO₃ solution, followed by two 10 ml washes with H₂O. After irradiation of 500 μ l of [¹⁸O]water with 10 MeV protons, the contents of the target were passed over the cartridge. The cartridge was rinsed with 3 ml water and [¹⁸F]fluoride was eluted with a solution of 7.5 mg kryptofix[®] 222 and 750 μ g K₂CO₃ in 0.75 ml of methanol/H₂O (90:10 v/v). The eluate was heated under argon flow at 98°C for 5 min to evaporate H₂O and methanol. Anhydrous acetonitrile (1 ml) was added twice and after each addition the acetonitrile was evaporated at 98°C under argon flow for 5 min. To the residue was added a solution of 5 mg of the precursor for labelling in 1.7 ml of anhydrous acetonitrile. The reaction mixture was heated at 85°C for 5 min in a closed vial. After cooling to room temperature, 10 ml of diethylether was added and the solution was passed over two Seppak[®] Plus silica cartridges (Waters). After evaporation of the solvent under argon flow, the residue was redissolved in 1 ml ethanol (EtOH). For RP-HPLC purification, the solution was applied on an Econosphere C18 10 μ m column (10 mm \times 250 mm, Alltech), eluted with a mixture of ethanol/0.1% ammonium acetate (50:50 v/v) at a flow rate of 3 ml/min. Specific activity was determined using a calibration curve obtained from the UV absorption (365 nm) of the cold compounds. For the calibration curve, different concentrations of a solution of **2** or **3** in acetonitrile were analyzed by RP-HPLC and the area under the curve was determined.

Partition coefficient determination

The lipophilicity of the RP-HPLC isolated fluorine-18 labelled compounds was determined using a modification of the method described by Yamauchi and co-workers.²⁹ In a test tube, 25 μ l of the RP-HPLC isolated fluorine-18 labelled compound was added to a mixture of 3 ml each of 1-octanol and 0.025 M phosphate buffer pH 7.4. The test tube was vortexed at room temperature for 2 min and then centrifuged at 2700 g for 10 min. A 100 μ l aliquot was taken from the octanol phase and a 900 μ l aliquot from the aqueous phase, taking care to avoid cross-contamination between the phases, and the aliquots were weighed. Their activity was counted using an automatic gamma counter and the partition coefficient P was calculated using the equation:

$$P = \frac{\text{cpm/ml octanol}}{\text{cpm/ml buffer}}$$

with cpm = counts per minute

Experiments were performed at least in triplicate.

Biodistribution in control mice

The radiometric peak on RP-HPLC containing the desired radiolabelled compound was collected and heated in an oil bath at 40°C under a nitrogen flow for 10 min. The residue was diluted with saline to adjust the radioactivity concentration to about 3.7 MBq/ml. Gas chromatography was used to verify that the concentration of ethanol was below 10%. Male NMRI mice were sedated by intraperitoneal injection of 0.75 μ l of a 1/4 dilution of Hypnorm[®] (fentanyl citrate 63 μ g/ml + fluanisone 2 mg/ml after dilution, Janssen-Cilag, Beerse, Belgium). An aliquot of 0.1 ml of one of the fluorine-18 labelled compounds (370 kBq) was injected via a tail vein. After decapitation at 2 or 60 min post-injection (p.i., four mice at each time point), blood was collected in tared tubes and weighed. All organs and other body parts were dissected and weighed and their activity was counted using an automatic gamma counter. Results were corrected for background activity and are expressed as percentage of the injected dose (% ID), equal to the sum of the activities in all organs except the tail, and as percentage of the injected dose per gram tissue (% ID/g). For calculation of the total activity in blood, blood mass was assumed to be 7 % of total body mass.³¹

In vitro affinity for human fibrillar amyloid β

Preparation of brain tissue homogenates

Post mortem brain tissues were obtained from four AD patients and four age-matched control persons at autopsy, and neuropathological diagnosis was confirmed by current criteria (NIA-Reagan Institute Consensus Group, 1997). The cerebellum and the affected temporal or parietal cortex of AD patients together with the corresponding regions from control persons were isolated. Gray matter was carefully separated from white matter from the cortical tissues. Homogenates were then prepared in phosphate buffered saline (PBS, pH 7.4) at a concentration of approximately 100 mg wet tissue/ml (motor-driven glass homogenizer for 30 s). The homogenates were aliquoted into 1 ml portions and stored at -70°C for 3–6 months without loss of binding signal.

Binding studies

Binding assays were carried out according to a method described previously³² using [¹²⁵I]IMPY (6-iodo-2-(4'-dimethylamino)phenyl-imidazo^{1,2} pyridine) with a specific activity of 81.4 TBq/mmol and more than 95% radiochemical purity.²³ Binding assays were carried out in 12 mm \times 75 mm borosilicate glass tubes. For saturation studies, the reaction mixture contained 50 μ l of *post mortem* AD brain homogenate (20–50 μ g), 50 μ l of an [¹²⁵I]IMPY solution in PBS (0.02–0.04 nM) and 40 μ l of a solution of the test compound (**2** and **3**; 10⁻⁷–10⁻¹⁰ M diluted serially in PBS containing 0.1 % bovine serum albumin) in a final volume of 1 ml. Non-specific binding was defined in the presence of 600 nM non-radioactive IMPY in the same assay tubes. For the competition binding studies, concentrations of 10⁻⁵–10⁻¹⁰ M of the compounds and 0.06 nM [¹²⁵I]IMPY were used. The mixtures were incubated at 37°C for 2 h, and the bound and the free radioactivity were separated by vacuum filtration through Whatman GF/B filters using a Brandel M-24R cell harvester (London, England) followed by two 3 ml

washes with PBS at room temperature. Filters containing the bound iodine-125 ligand were counted in a gamma counter (Packard 5000, Ramsey, Minnesota, USA) with 70% counting efficiency. Under the assay conditions, the specifically bound fraction was less than 15% of the total radioactivity. Protein determinations were performed with Lowry's method using bovine serum albumin as a standard.³³ The results of saturation and inhibition experiments were subjected to non-linear regression analysis using EBDA by which K_d and K_i values were calculated.

In vitro affinity for amyloid present in mouse brain sections

Transgenic mice overexpressing human A β PP (London mutation, >12 months old) were anaesthetized with pentobarbital and the brain was flushed transcardially with icecold saline. The brain was removed and post-fixed overnight with 4% paraformaldehyde in PBS. One part of the brain was stored in 0.1% sodium azide in PBS at 4°C. The other part was processed for paraffin embedding. 6 μ m sagittal sections were cut using a Microm HM 340 E microtome (Microm, Walldorf, Germany). Prior to incubation, paraffin sections were taken through two 5 min washes with xylol, followed by 1 min sequential washes with 100, 100, 90, 70, 50% ethanol and PBS before they were blow-dried. After rehydration, the sections were incubated for 1 h with one of the cold compounds (**2** or **3**) in a concentration range between 10 μ M and 10 nM. After 1 h, the brain sections were rinsed with tap water and coverslipped with a Mowiol-DABCO solution (Calbiochem, Darmstadt, Germany). For immunohistochemical staining, the same deparaffinization protocol was used. The sections were pretreated with 96% formic acid for 7 min to enhance signal. After rinsing with PBS, the sections were treated with 1.5% H₂O₂ in PBS/methanol 50:50 v/v to inhibit endogenous peroxidase. Non-specific binding was blocked by treatment with PBS containing 0.05% tween[®] 20 (PBST) and 10% fetal calf serum (FCS, Gentaur, Brussels, Belgium). The sections were incubated overnight with pan β -amyloid (AB-1) polyclonal antibodies (Oncogene Research Products, San Diego, CA, USA) diluted 1/1000 in PBST 10% FCS at 4°C. After rinsing in PBST, the sections were incubated for 1 h with 1/500 diluted goat anti-rabbit biotin (Vector Laboratories, Burlingame, CA, USA) in PBST 10% FCS. Then, sections were incubated with avidin biotin complex (Vectastain Elite ABC-peroxidase kit, Vector Laboratories) dissolved in PBST 10% FCS for 30 min at room temperature. Peroxidase activity was developed with 3,3'-diaminobenzidine, after which the sections were counterstained with hematoxylin. In case no immunohistochemical staining was done, the presence of plaques in the transgenic mice was confirmed by incubation of neighbouring sections with X-34. Fluorescence microscopy was performed using a Leica DMR microscope equipped with a digital Leica DC480 camera (Leica Microsystems, Groot Bijgaarden, Belgium) and a UV filter set with following specifications: excitation: 340–380 nm bandpass filter, dichromatic mirror 400 nm; emission: 425 nm longpass filter. The images were acquired and processed with Leica IM500 image processing software.

Conclusion

Two 2-(4'-aminophenyl)-1,3-benzothiazoles were derivatized either at the 6-position or at the 2'-position with a tosyloxypropoxy moiety and then labelled with ¹⁸F in a 50% yield, resulting in an average specific activity of about 42 GBq/ μ mol EOS. Identity confirmation of the ¹⁸F-labelled phenylbenzothiazole derivatives

was done using radio-LC-MS and by comparison of retention times on RP-HPLC. The partition coefficient of the two compounds is compatible with a free passive diffusion over the BBB. In control mice both compounds have a relatively high initial brain uptake, which is significantly higher for [¹⁸F]**2** (2 min p.i.: [¹⁸F]**2**: 4.5% ID/g and [¹⁸F]**3**: 3.0% ID/g, $p < 0.05$), whereas wash-out from control brain is faster for [¹⁸F]**3**. *In vitro* binding affinity tests using *post mortem* human AD brain homogenates revealed that only compound **2** has affinity for fibrillar amyloid β . This was confirmed by incubation of APP mouse brain sections with the cold compounds, where **3** did not stain any structure while **2** stained amyloid plaques present in APP mouse brain. These data suggest that [¹⁸F]**2** may be a useful tracer for *in vivo* visualization of fibrillar amyloid β .

REFERENCES

- [1] L. Cai, R. B. Innis, V. W. Pike, *Curr Med Chem* **2007**, *4*, 19–52.
- [2] W. E. Klunk, M. L. Debnath, J. W. Pettegrew, *Neurobiol Aging* **1994**, *15*, 691–698.
- [3] S. D. Styren, R. L. Hamilton, G. C. Styren, W. E. Klunk, *J Histochem Cytochem* **2000**, *48*, 1223–1232.
- [4] D. M. Skovronsky, B. Zhang, M. P. Kung, H. F. Kung, J. Q. Trojanowski, VM-Y. Lee, *Proc Natl Acad Sci USA* **2000**, *97*, 7609–7614.
- [5] M. L. Schmidt, T. Schuck, S. Sheridan, M. P. Kung, H. Kung, Z. P. Zhuang, *Am J Pathol* **2001**, *159*, 937–943.
- [6] C-W. Lee, Z-P. Zhuang, M-P. Kung, K. Plössl, D. Skovronsky, T. L. Gur, *J Med Chem* **2001**, *44*, 2270–2275.
- [7] Z-P. Zhuang, M-P. Kung, C. Hou, D. Skovronsky, T. L. Gur, K. Plössl, *J Med Chem* **2001**, *44*, 1905–1914.
- [8] M. Ono, A. Wilson, J. Nobrega, D. Westaway, P. Verhoeff, Z-P. Zhuang, *Nucl Med Biol* **2003**, *30*, 565–571.
- [9] H. Kung, C. Lee, Z. Zhuang, M. Kung, C. Hou, K. Plössl, *J Am Chem Soc* **2001**, *123*, 12740–12741.
- [10] E. D. Agdeppa, V. Kepe, J. Liu, S. Flores-Torres, N. Satyamurthy, A. Petric, *J Neurosci* **2001**, *21*, RC189.
- [11] K. Shoghi-Jadid, G. W. Small, E. D. Agdeppa, V. Kepe, L. M. Ercoli, P. Siddarth, *Am J Geriatr Psychiatry* **2002**, *10*, 24–35.
- [12] C-W. Lee, M-P. Kung, C. Hou, H. F. Kung, *Nucl Med Biol* **2003**, *30*, 573–580.
- [13] N. Okamura, T. Suemoto, H. Shimadzu, M. Suzuki, T. Shiomiitsu, H. Akatsu, *J Neurosci* **2004**, *24*, 2535–2541.
- [14] T. Suemoto, N. Okamura, T. Shiomiitsu, M. Suzuki, H. Shimadzu, H. Akatsu, *Neurosci Res* **2004**, *48*, 65–74.
- [15] C. C. Rowe, U. Ackerman, W. Browne, R. Mulligan, K. L. Pike, G. O'Keefe, H. Tochon-Danguy, G. Chan, S. U. Berlangieri, G. Jones, K. L. Dickinson-Rowe, H. P. Kung, W. Zhang, M. P. Kung, D. Skovronsky, F. Dyrks, G. Holl, S. Krause, M. Friebe, L. Lehman, S. Lindeman, L. M. Dinkelborg, C. L. Masters, V. L. Villemagne, *Lancet Neurol* **2008**, *7*, 129–135.
- [16] W. E. Klunk, Y. Wang, G-F. Huang, M. L. Debnath, D. P. Holt, C. A. Mathis, *Life Sci* **2001**, *69*, 1471–1484.
- [17] Y. Wang, W. E. Klunk, G-F. Huang, M. L. Debnath, D. P. Holt, C. A. Mathis, *J Mol Neurosci* **2002**, *19*, 11–16.
- [18] C. A. Mathis, B. J. Bacskai, S. T. Kajdasz, M. E. McLellan, M. P. Frosch, B. T. Hyman, *Bioorg Med Chem Lett* **2002**, *12*, 295–298.
- [19] C. A. Mathis, Y. Wang, D. P. Holt, G-F. Huang, M. L. Debnath, W. E. Klunk, *J Med Chem* **2003**, *46*, 2740–2754.
- [20] Z-P. Zhuang, M-P. Kung, C. Hou, K. Plössl, D. Skovronsky, T. L. Gur, *Nucl Med Biol* **2001**, *28*, 887–894.
- [21] M. Ono, M-P. Kung, C. Hou, H. F. Kung, *Nucl Med Biol* **2002**, *29*, 633–642.
- [22] M-P. Kung, C. Hou, Z-P. Zhuang, B. Zhang, D. Skovronsky, J. Q. Trojanowski, *Brain Res* **2002**, *956*, 202–210.
- [23] M-P. Kung, C. Hou, Z-P. Zhuang, A. J. Cross, D. L. Maier, H. F. Kung, *Eur J Nucl Med Mol Imaging* **2004**, *31*, 1136–1145.
- [24] C. Mathis, B. Lopresti, N. Mason, J. Price, N. Flatt, W. Bi, S. Ziolkowski, S. DeKosky, W. J. Klunk, *J Nucl Med* **2007**, *48*, 56P.

- [25] K. Serdons, T. Verduyck, D. Vanderghinste, J. Cleynhens, P. Borghgraef, P. Vermaelen, C. Terwinghe, F. Van Leuven, K. Van Laere, H. Kung, G. Bormans, A. Verbruggen, *Bioorg Med Chem Lett* **2009**, *19*, 602–605.
- [26] K. Serdons, C. Terwinghe, P. Vermaelen, K. Van Laere, H. Kung, L. Mortelmans, G. Bormans, A. Verbruggen, *J Med Chem* **2009**, *52*, 1428–1437.
- [27] D-F. Shi, T. D. Bradshaw, S. Wrigley, C. J. McCall, P. Lelieveld, I. Fichtner, *J Med Chem* **1996**, *39*, 3375–3384.
- [28] Y. Zea-Ponce, S. Mavel, T. Assaad, S. E. Kruse, S. M. Parsons, P. Emond, S. Chalon, N. Giboureau, M. Kassiou, D. Guilloteau, *Bioorg Med Chem* **2005**, *13*, 745–753.
- [29] H. Yamauchi, J. Takahashi, S. Seri, H. Kawashima, H. Koike, M. Kato-Azuma In *Technetium and Rhenium in Chemistry and Nuclear Medicine*, Vol. 3 (Eds.: M. Nicolini, G. Bandoli, U. Mazzi), Cortina International, Verona, Italy, **1989**, pp. 475–502.
- [30] D. D. Dishino, M. J. Welch, M. R. Kilbourn, M. E. Raichle, *J Nucl Med* **1983**, *24*, 1030–1038.
- [31] A. Fritzberg, W. Whitney, C. Kuni, W. Klingensmith, *Int J Nucl Med Biol* **1982**, *9*, 79–82.
- [32] M. P. Kung, C. Hou, Z. P. Zhuang, D. Skovronsky, H. F. Kung, *Brain Res* **2004**, *1025*, 89–105.
- [33] P. J. Munson, D. Rodbard, *Anal Biochem* **1980**, *107*, 220–239.